

## Temporal variance of lower mesospheric ozone over Switzerland during winter 2000/2001

Klemens Hocke,<sup>1</sup> Niklaus Kämpfer,<sup>1</sup> Dietrich G. Feist,<sup>1</sup> Yasmine Calisesi,<sup>2</sup> Jonathan H. Jiang,<sup>3</sup> and Simon Chabrilat<sup>4,5</sup>

Received 15 December 2005; revised 24 March 2006; accepted 29 March 2006; published 2 May 2006.

[1] The Stratospheric Ozone Monitoring Radiometer (SOMORA) is continuously operated in Switzerland and measures ozone volume mixing ratio  $q_{O_3}$  in the stratosphere and lower mesosphere with a time resolution of about 30 min. Temporal variances  $S$  (wave period band 1–3 h) of daytime and nighttime ozone are studied at an altitude of 55 km from October 1, 2000 to May 1, 2001. Gravity waves are assumed as cause of the observed short-time fluctuations of  $q_{O_3}$ . Strong negative and positive correlations are found between the dynamic state of the stratosphere (represented by time series of ERA-40 reanalyses) and SOMORA's  $S$  and  $q_{O_3}$  series of lower mesospheric ozone. Oscillations with periods of 5–30 days are present in the  $S$  and  $q_{O_3}$  series. **Citation:** Hocke, K., N. Kämpfer, D. G. Feist, Y. Calisesi, J. H. Jiang, and S. Chabrilat (2006), Temporal variance of lower mesospheric ozone over Switzerland during winter 2000/2001, *Geophys. Res. Lett.*, 33, L09801, doi:10.1029/2005GL025496.

### 1. Introduction

[2] The present study takes advantage of the relatively high time resolution and completeness of the ozone time series recorded by the SOMORA microwave radiometer [Calisesi, 2003] in Switzerland. Midlatitude gravity waves produce periodic fluctuations of ozone volume mixing ratio  $q_{O_3}$  in the upper stratosphere and lower mesosphere. The most relevant process is possibly the vertical advection of air parcels by gravity waves [Zhu and Holton, 1986]. Because of the negative vertical gradient of  $q_{O_3}$ , an ascending (descending) air parcel has a larger (smaller)  $q_{O_3}$  than its environment at a fixed altitude. During daytime, the temperature dependence of reaction rate coefficients is expected to enhance gravity-wave induced  $q_{O_3}$  fluctuations. In the present study, short-time fluctuations (period band 1–3 h) of  $q_{O_3}$  are derived from SOMORA data of the winter season 2000/2001. The variance of the relative  $q_{O_3}$  fluctuations may represent the temporal variance of gravity waves at lower mesospheric altitudes.

<sup>1</sup>Institute of Applied Physics, University of Bern, Bern, Switzerland.

<sup>2</sup>International Space Science Institute, Bern, Switzerland.

<sup>3</sup>Jet Propulsion Laboratory, California Institute of Technology, Pasadena, California, USA.

<sup>4</sup>Meteorological Service of Canada, Dorval, Quebec, Canada.

<sup>5</sup>On leave from Belgian Institute for Space Aeronomy, Brussels, Belgium.

### 2. Measurement and Data Analysis

#### 2.1. SOMORA Ozone Radiometer

[3] The stratospheric ozone monitoring radiometer (SOMORA) monitors the radiation of the thermal emission of ozone at 142.175 GHz. SOMORA has been developed at the Institute of Applied Physics, University Bern. The instrument was first put into operation on January 1, 2000 and was operated in Bern (46.95 N, 7.44 E) until May 2002. In June 2002, the instrument was moved to Payerne (46.82 N, 6.95 E) where its operation has been taken over by MeteoSwiss. SOMORA contributes primary data to the Network for Detection of Stratospheric Change (NDSC).

[4] The vertical distribution of ozone is retrieved from the recorded pressure-broadened ozone emission spectra by means of the optimal estimation method [Rodgers, 1976]. A radiative transfer model is used to compute the expected ozone emission spectrum at the ground. Beyond 45 km altitude, the model atmosphere is based on monthly averages of temperature and pressure of the CIRA-86 climatology, adjusted to actual ground values using the hydrostatic equilibrium equation. Either a winter or summer CIRA-86 ozone profile is taken as a priori. The retrieved profiles minimize a cost function that includes terms in both the measurement and state space. The altitude  $h$  is fixed in both the forward and inverse models, and altitude-dependent information is extracted from the measured spectra by reference to the pressure profile used. SOMORA retrieves  $q_{O_3}$  with less than 20% a priori contribution in the 25 to 65 km altitude range, with a vertical resolution of 8–10 km, and a time resolution (spectra integration time) of  $\sim 30$  min. More details concerning the instrument design, data retrieval, and intercomparison are given by Calisesi [2000], Calisesi [2003], and Calisesi et al. [2005].

#### 2.2. Fluctuations of Ozone Volume Mixing Ratio

[5] Zhu and Holton [1986] emphasize that vertical parcel advection of ozone gives a negative correlation between ozone caused heating and temperature perturbations. This phenomenon is called *photochemical damping of gravity waves* and stabilizes the upper stratosphere and lower mesosphere. In the following, we analyze the relative fluctuations of  $q_{O_3}(t)$  at  $h = 55$  km. The selected altitude is beyond the stratopause and within the altitude range where the SOMORA ozone profile mainly depends on the measured spectrum (contribution of the a priori profile is around 20% at  $h = 55$  km). Results remain similar if the altitude is changed by some 2–3 km. The SOMORA time series is almost continuous from October 1, 2000 to May 1, 2001, however some days with data gaps occurred. 88% of the data points within the selected time interval have a temporal spacing between 29 and 31 min. For band pass

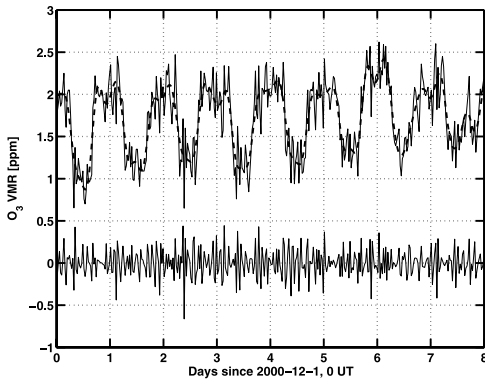


**Figure 1.** Ozone volume mixing ratio observed by the SOMORA radiometer at  $h = 55$  km over Bern (46.95 N, 7.44 E) during December 1–8, 2000 (upper solid line). The 6-hour low pass filtered series (dashed line) is superposed. The band pass filtered series (lower solid line) denotes the ozone fluctuations in the period band 1 to 3 hours.

filtering, the ozone time series is linearly interpolated on a grid with a fixed time step of 30 min. Then the ozone time series is filtered by a digital nonrecursive low pass and band pass hamming filter in forward and reverse direction. The period range of the band pass is from 1 to 3 hours, and the low pass filter is open for wave periods  $>6$  hours. Figure 1 shows for example the result of the time interval 1–8 December 2000. The original series is the solid line with large, nighttime  $q_{O_3}$  and small daytime  $q_{O_3}$  values. The low-pass filtered series  $\bar{q}_{O_3}(t)$  is superposed and denoted by the dashed line. The bandpass filtered time series  $\Delta q_{O_3}(t)$  consists of the high-frequency fluctuations (periods 1–3 h, solid line at the bottom of the graph). In the following, the series  $\Delta q_{O_3}(t)$  and  $\bar{q}_{O_3}(t)$  are divided into daytime series ( $\Delta q_{O_3,day}(t)$ ,  $\bar{q}_{O_3,day}(t)$  for solar zenith angle  $SZA(t) < 97.5^\circ = 180^\circ - \arcsin(\frac{r_E - h}{r_E + h})$  with  $h = 55$  km) and nighttime series ( $\Delta q_{O_3,night}(t)$ ,  $\bar{q}_{O_3,night}(t)$  for  $SZA(t) > 97.5^\circ$ ).

### 3. Results

#### 3.1. Temporal Variance of Ozone

[6] The variance  $S$  is a useful parameter for the description of the power contained in the short-time (1–3 h) fluctuations of  $q_{O_3}$ . The daytime variance  $S_{day}$  of the relative  $q_{O_3}$  fluctuation series at data point  $i$  within an interval of length  $n$  is given by

$$S_{day}(i) = \frac{1}{n-1} \sum_{j=1}^n \left[ \frac{\Delta q_{O_3,day}(i+j-\frac{n}{2})}{\bar{q}_{O_3,day}(i+j-\frac{n}{2})} \right]^2. \quad (1)$$

[7] The nighttime variance  $S_{night}$  is calculated in a similar manner. The selected length of the data interval corresponds to half a day ( $n = 24$ ). The data gaps during day or night are ignored, for example, if the sunset occurs in the daytime series at data point  $i$ , the next data point  $i + 1$  is the first point after sunrise on the next day.

[8] Figures 2a and 2b show the results for  $S_{night}$  and  $S_{day}$ , respectively. 5 to 6-day modulations of  $S_{day}$  occur in mid of November and end of December. Three enhancements of  $S_{day}$  appear in mid of November, January, and February as indicated by the three gray boxes in Figure 2b.

[9] During winter 2000/2001 the mean value of  $S_{day}$  is around 0.02 corresponding to  $\Delta q_{O_3,day}/q_{O_3,day} = 14\%$ . The mean value of  $S_{night}$  is around 0.007 corresponding to  $\Delta q_{O_3,night}/q_{O_3,night} = 8\%$ . Now we briefly estimate if vertical advection of air parcels by gravity waves can explain the observed mean fluctuation amplitudes of  $\Delta q_{O_3}/q_{O_3}$ . The SOMORA radiometer observed vertical gradients ( $dq_{O_3}/dh)/q_{O_3}$  which are around  $-5\%/km$  during night and  $-8\%/km$  during day in December 2000 at  $h = 55$  km. The ozone volume mixing ratio shall remain constant in an ascending or descending air parcel (this assumption is at least justified during nighttime since photodissociation disappears). The  $q_{O_3}$  fluctuation due to vertical parcel advection by a gravity wave (gw) is given by

$$\frac{\Delta q_{O_3,gw}}{q_{O_3,gw}} = \frac{dq_{O_3}/dh}{q_{O_3}} \left( \frac{2\Delta w}{\pi} \right) \frac{T_p}{2}. \quad (2)$$

[10] For a medium-scale gravity wave at lower mesospheric heights, a vertical velocity amplitude  $\Delta w = 1$  m/s and a period  $T_p = 1$  hour can be considered. Inserting all values in equation (2) we get at  $h = 55$  km:  $(\Delta q_{O_3,gw,day})/q_{O_3,gw,day} = 9\%$  and  $(\Delta q_{O_3,gw,night})/q_{O_3,gw,night} = 6\%$  which are of the same order as the mean fluctuation amplitudes observed by SOMORA. This rough estimation shows that a connection between gravity wave variance and ozone variance is reasonable at lower mesospheric heights. During daytime, photochemical reactions inside the ascending and descending air parcels are expected to enhance the  $q_{O_3}$  fluctuation amplitude during the passage of a gravity wave. In particular the destruction of  $O_3$  by recombination with  $O$  is decreased in an ascending air parcel with adiabatic temperature decrease [Eckermann et al., 1998]. The temperature dependence of the ozone destruction process always gives a negative correlation between the  $q_{O_3}$  variation and the temperature perturbation. According to Zhu and Holton [1986] this is the major process for variations of  $q_{O_3}$  caused by long-time temperature oscillations (e.g., due to traveling planetary waves). Calisesi et al. [2001] find a negative correlation  $r = -0.7$  between such variations of temperature and  $q_{O_3}$  in the wintertime upper stratosphere over Bern.

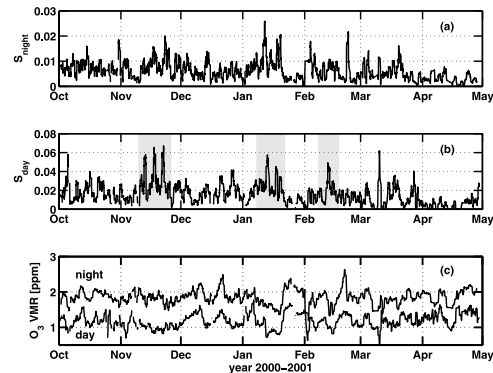


**Figure 2.** (a) Nighttime and (b) daytime variances  $S$  (period band 1–3 h) of ozone vmr at  $h = 55$  km over Bern. (c) Nighttime and daytime ozone volume mixing ratio (0.5-day average) for the time from October 1, 2000 to May 1, 2001.

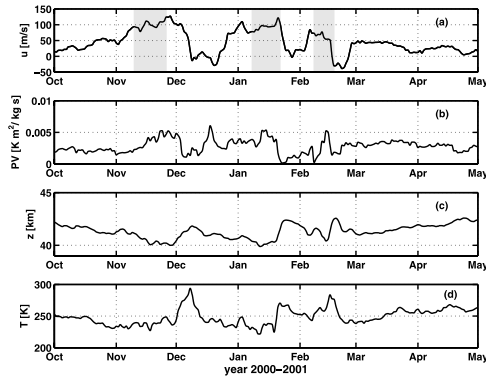


**Figure 3.** ERA-40 reanalyses at pressure level  $p = 2.08$  hPa from October 1, 2000 to May 1, 2001: (a) eastward wind  $u$ , (b) potential vorticity  $PV$ , (c) pressure level height  $z$ , and (d) temperature  $T$ .

[11] The moving half-day averages of the low pass filtered series  $\bar{q}_{O_3,day}$  and  $\bar{q}_{O_3,night}$  are shown in Figure 2c for comparison with the short-time variance in Figures 2a and 2b. From December to March, variations with periods of 10–20 days appear in both series of  $O_3$  which might be linked to traveling planetary waves. The enhancements of the variance in Figure 2b seem to precede the onset of planetary-wave like oscillations in Figure 2c. *Jacobi et al.* [2003] observed planetary-wave oscillations with periods of 10 and 20 days in the upper mesospheric and lower thermospheric wind fields over Europe from January to March 2001. They interpret the observations by a 10-day planetary wave with upward energy propagation and a 20-day oscillation with relative constant phase, related to the major stratospheric warming in mid of February 2001.

### 3.2. Dynamic State of the Stratosphere

[12] The meteorological situation of the stratosphere during the winter 2000/2001 is represented by means of the ERA-40 reanalyses of ECMWF (European Center for Medium-range Weather Forecast). Figure 3 shows the highly variable time series of eastward wind  $u$ , potential vorticity  $PV$ , pressure level height  $z$ , and temperature  $T$  at the pressure level  $p = 2.08$  hPa for the location of Bern. The eastward wind  $u$  reaches speeds of around 100 m/s at end of November, mid January, and beginning of February (indicated by the gray boxes, same position as in Figure 2b). Sudden reversals from eastward to westward direction occur in mid December, end of January, and end of February. A major stratospheric warming is present in mid of February 2001, most obvious in the time series of  $PV$  and  $T$ .

### 3.3. Correlation Between the Stratosphere and the Lower Mesosphere

[13] We investigate in how far the temporal variance of lower mesospheric ozone is correlated with the dynamic state of the stratosphere over Bern. A 14-day moving average is applied to the ERA-40 time series of  $u$ ,  $v$ ,  $z$ ,  $T$ , and potential vorticity  $PV$  as well as to SOMORA's time series of variance  $S_{day}$ ,  $S_{night}$ , and ozone mixing ratios  $q_{O_3,day}$  and  $q_{O_3,night}$  (correlations seem to be maximal for a data window length of 14 days). Some of the averaged time series are depicted in Figure 4. For a complete overview, the correlation coefficient  $r$  is given for all

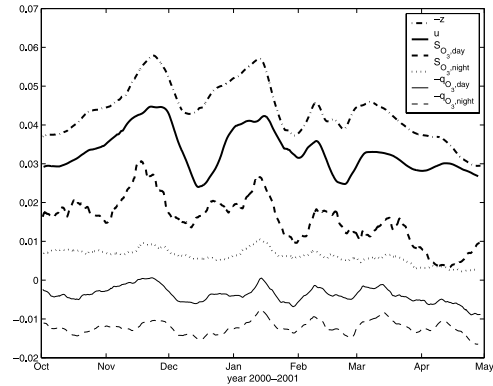


**Figure 4.** A 14-day moving average is applied to the time series pressure level height  $z$  (dash-dotted line, ERA-40 reanalyses at  $p = 2.08$  hPa), eastward wind  $u$  (thick solid line, ERA-40 reanalyses at  $p = 2.08$  hPa), daytime ozone variance  $S_{O_3,day}(h = 55$  km) (thick dashed line), nighttime ozone variance  $S_{O_3,night}(h = 55$  km) (dotted line), daytime ozone VMR  $-q_{O_3,day}(h = 55$  km) (thin solid line), and nighttime ozone VMR  $-q_{O_3,night}(h = 55$  km) (thin dashed line) from October 1, 2000 to May 1, 2001. The  $-z$ ,  $u$ , and  $-q_{O_3}$  series are scaled and vertically shifted while the  $y$ -axis is true for the  $S_{day}$  and  $S_{night}$  series.

relevant cross correlations between the ERA-40 series and SOMORA's ozone series in Table 1. Two values of  $r$  are given, the first refers to the ERA-40 series at  $p = 2.08$  hPa ( $\sim 40$  km) while the second ( $r$  in brackets) refers to the ERA-40 series at  $p = 9.89$  hPa ( $\sim 30$  km). Strong negative and positive correlations exist between eastward wind  $u$ , pressure level height  $z$ , temperature  $T$ , variance  $S$ , and mixing ratio  $q_{O_3}$ . Weaker correlations are found for the series of potential vorticity  $PV$  and northward wind  $v$ . Generally the correlation  $r$  is stronger for the ERA-40 series at the upper pressure level  $p = 2.08$  hPa which is closer to the ozone measurement altitude  $h = 55$  km. A remarkable exception is the  $T$  series showing higher absolute values of  $r$  at the lower pressure level  $p = 9.89$  hPa. The dynamic parameters  $u$ ,  $z$ , and  $T$  are connected by the primitive equations of atmospheric dynamics, and we may concentrate on the correlation between eastward wind  $u$  and variance  $S$ .

**Table 1.** Correlation Coefficient  $r^a$

	$S_{day}$	$S_{night}$	$q_{O_3,day}$	$q_{O_3,night}$
$u$	0.68(0.51)	0.70(0.55)	-0.71(-0.54)	-0.54(-0.43)
$v$	0.32(0.12)	0.32(0.00)	-0.25(-0.21)	-0.14(-0.02)
$z$	-0.82(-0.67)	-0.75(-0.63)	0.79(0.60)	0.46(0.41)
$T$	-0.66(-0.77)	-0.59(-0.68)	0.63(0.67)	0.26(0.37)
$PV$	0.41(-0.05)	0.26(-0.10)	-0.49(0.10)	-0.42(0.01)
$q_{O_3,day}$	-0.75	-0.74	-	0.70
$q_{O_3,night}$	-0.27	-0.46	-	-
$S_{night}$	0.88	-	-	-

<sup>a</sup>ERA-40 series  $u$ ,  $v$ ,  $z$ ,  $T$ , and  $PV$  are at pressure level 2.08 hPa ( $z \sim 40$  km). The  $r$ -values of pressure level  $p = 9.89$  hPa ( $z \sim 30$  km) are given in the parentheses. Ozone variances  $S$  and ozone volume mixing ratios  $q_{O_3}$  are at 55 km altitude. A 14-day moving average has been applied to all series from 2000-10-1 to 2001-5-1.



### 3.3.1. Zonal Wind and Ozone Variance

[14] At midlatitudes during wintertime, the zonal wind often has an eastward direction from the surface to the mesosphere. This condition allows an upward propagation of gravity waves and planetary waves traveling westward against the eastward wind from the troposphere to the mesosphere. Critical level filtering of gravity waves possibly explain the strong positive correlation ( $r = 0.70$ ) between the eastward stratospheric wind and the lower mesospheric ozone variance (Table 1). If the zonal wind reverses from eastward to westward direction, westward propagating gravity waves from below are blocked by the critical level in the stratosphere. Consequently the ozone distribution of the lower mesosphere is less disturbed, and the variance  $S$  is reduced (e.g., mid of December in Figure 4).

### 3.3.2. Ozone Volume Mixing Ratio and Ozone Variance

[15] A strong negative correlation of  $r = -0.75$  is found between the ozone volume mixing ratio  $q_{O_3}$  and the ozone variance  $S$  during daytime (Table 1). Mixing of the atmosphere by gravity waves may lead to enhanced destruction of odd oxygen by reactions with  $NO_x$ ,  $ClO_x$ , and  $HO_x$ . This may explain the decrease of  $q_{O_3}$  when the ozone variance  $S$  increases.

## 4. Concluding Remarks

[16] The temporal variance of the ozone volume mixing ratio  $q_{O_3}$  has been analyzed by using SOMORA microwave radiometer data of the lower mesosphere with a time resolution of 30 min. Because of the negative vertical gradient of  $q_{O_3}$  in the lower mesosphere, gravity wave-induced vertical parcel advection may generate short-time fluctuations in the time series of  $q_{O_3}$ . A positive correlation ( $r = 0.70$  during night) is found between the eastward stratospheric wind  $u$  and the lower mesospheric ozone variance  $S$  during the winter 2000/2001. The highly variable zonal wind field of the stratosphere seems to modulate the upward gravity wave momentum flux by critical level filtering. SOMORA's time series of  $q_{O_3}$  and  $S$  contain a manifold of oscillations from 5 to 30 days which are probably associated with traveling planetary waves. A

strong negative correlation is observed between  $q_{O_3}$  and  $S$  during daytime ( $r = -0.75$ ). Ground-based microwave radiometry of ozone seems to be an efficient tool for monitoring of the dynamic coupling between the stratosphere and the mesosphere.

[17] **Acknowledgments.** This work has been funded by MeteoSwiss within the Swiss GAW program. We thank the reviewers for many constructive advises and improvements. The ERA-40 reanalyses data have been provided by ECMWF's Meteorological Archival and Retrieval System.

## References

- Calisesi, Y. (2000), Monitoring of stratospheric and mesospheric ozone with a ground-based microwave radiometer: Data retrieval, analysis, and applications, Ph.D. thesis, Philos.Naturwiss. Fak., Univ. Bern, Bern, Switzerland. (Available at <http://www.iap.unibe.ch/publications/>.)
- Calisesi, Y. (2003), The Stratospheric Ozone Monitoring Radiometer SOMORA: NDSC Application Document, *IAP Res. Rep.2003-11*, Inst. für Angewandte Phys., Univ. Bern, Bern, Switzerland. (Available at <http://www.iap.unibe.ch/publications/>.)
- Calisesi, Y., H. Wernli, and N. Kämpfer (2001), Midstratospheric ozone variability over Bern related to planetary wave activity during the winters 1994–1995 to 1998–1999, *J. Geophys. Res.*, *106*, 7903–7916.
- Calisesi, Y., V. T. Soebijanta, and R. O. van Oss (2005), Regridding of remote soundings: Formulation and application to ozone profile comparison, *J. Geophys. Res.*, *110*, D23306, doi:10.1029/2005JD006122.
- Eckermann, S. D., D. E. Gibson-Wilde, and J. T. Bacmeister (1998), Gravity wave perturbations of minor constituents: A parcel advection methodology, *J. Atmos. Sci.*, *55*, 3521–3539.
- Jacobi, C., D. Kürschner, H. Müller, D. Pancheva, N. J. Mitchell, and B. Naujokat (2003), Response of the mesopause region dynamics to the February 2001 stratospheric warming, *J. Atmos. Sol. Terr. Phys.*, *65*, 834–855.
- Rodgers, C. D. (1976), Retrieval of atmospheric temperature and composition from remote measurements of thermal radiation, *Rev. Geophys.*, *14*, 609–624.
- Zhu, X., and J. R. Holton (1986), Photochemical damping of inertia-gravity waves, *J. Atmos. Sci.*, *43*, 2578–2584.
- Y. Calisesi, International Space Science Institute, Hallerstrasse 6, CH-3012 Bern, Switzerland.
- S. Chabrilat, Meteorological Service of Canada, QC, Dorval, Canada H9P 1J3.
- D. G. Feist, K. Hocke, and N. Kämpfer, Institute of Applied Physics, University of Bern, CH-3012 Bern, Switzerland. (klemens.hocke@mw.iap.unibe.ch)
- J. H. Jiang, Jet Propulsion Laboratory, California Institute of Technology, Mail Stop 183-701, 4800 Oak Grove Drive, Pasadena, CA 91109–8099, USA.